Sol−Gel Trapping of Functional Intermediates of Hemoglobin: Geminate and Bimolecular Recombination Studies†

Imran Khan, Colman F. Shannon, David Dantsker, Adam J. Friedman, Jose Perez-Gonzalez-de-Apodaca, and Joel M. Friedman*

Department of Physiology and Biophysics, Albert Einstein College of Medicine, Bronx, New York 10461

Received March 8, 2000; Revised Manuscript Received June 29, 2000

ABSTRACT: The encapsulation of proteins in porous sol−gels is a promising technique for generating, trapping, and probing functionally significant nonequilibrium protein species. An essential step needed in the pursuit of that goal is establishing the degree to which the sol−gel limits conformational change upon adding or removing substrates. In the present study, geminate recombination and solvent phase bimolecular recombination of CO to human adult hemoglobin (HbA) are used as sensitive probes of the degree of conformational constraint within the sol−gel. Two forms of CO saturated encapsulated HbA are generated. In one case, designated [COHbA], the equilibrium form of COHbA is directly encapsulated. In the second case, designated as [deoxyHbA] + CO, the equilibrium form of deoxyHbA is encapsulated and only after the sample has aged is CO introduced to the HbA through the porous sol−gel matrix. Three different preparative protocols are used to generate the sol−gels for each of the two forms of encapsulated COHbA. The kinetic traces obtained from these encapsulated samples allow for an easy evaluation of the extent to which the sol−gel is locking in the initial tertiary/quaternary structure. The results show that the sol−gel encapsulated samples can be used with pulsed laser sources and that one of the tested encapsulation protocols is far superior with respect to conformational locking. This protocol is used to trap and probe nonequilibrium forms such as the liganded T state of HbA, a species whose properties are needed to fully explore allostery in HbA.

Cooperative ligand binding to hemoglobin is an important biophysical phenomenon that has been extensively studied (*1*−*11*). As a result, hemoglobin has become, in effect, a model system both for exploring general concepts such as allostery and protein dynamics and for developing new biophysical tools to probe protein behavior. In addition, despite the considerable effort directed toward the study of hemoglobin, many basic mechanistic questions regarding allostery remain unanswered. However, the extensive structural and functional database derived from these many studies provides an infrastructure for posing and addressing many of these detailed yet general biophysical questions. In this study, the use of a relatively new sol−gel-based method of trapping allosteric intermediates of hemoglobin is evaluated with respect to the ligand rebinding kinetics. The combination of kinetics and the sol−gel encapsulation technique offers the promise of characterizing the functional properties of nonequilibrium species such as those that contribute to the allosteric behavior of hemoglobin.

The functional form of adult human hemoglobin (HbA) is a tetramer derived from two stable identical heterodimers. Each dimer is made up of two different myoglobin-like subunits. The two different subunits are called α and β. Thus the tetramer is in effect a homodimer composed of two $\alpha\beta$ dimers ($\alpha_1\beta_1$ and $\alpha_2\beta_2$) with an oxygen binding heme in each of the four subunits. The tetramer has been shown to adopt two well-defined quaternary structures termed R and T. The expression quaternary state is often used to encompass the range of reactivity and conformational plasticity that falls within the parameters associated of the R and T quaternary structures. The global quaternary structure is intimately coupled to the tertiary structure at the $\alpha_1\beta_2$ and $\alpha_2\beta_1$ interfaces between the $\alpha_1\beta_1$ and $\alpha_2\beta_2$ dimers.

Many of the features of cooperative ligand binding to hemoglobin can be explained using models based on a ligand binding dependent equilibrium between two quaternary structures: the low-affinity T structure and the high-affinity R structure (*3*, *5*, *9*, *12*, *13*). The basic general picture states that when fully ligand free, the ferrous form of human adult hemoglobin (HbA) adopts the T quaternary structure. Ligand binding to a T state structure occurs with low affinity. When three of the four ferrous heme sites have bound ligands, the equilibrium shifts sufficiently toward the R structure that the remaining ligands bind with much higher affinity.

The physical and functional properties of the equilibrium populations of fully ligand free (deoxyHbA) and fully liganded HbA (e.g., COHbA or O_2HbA) have been well characterized. The properties of nonequilibrium species that participate in the R−T switching mechanism, including partially liganded intermediates, are much more difficult to study. Probing such intermediates is an essential element in the unraveling of molecular details behind allostery. What would be most helpful in pursuing this endeavor are methods

† This work was supported in part by the National Institutes of Health through Grants P01 HL5108 and R01 HL58247 and by the W. M. Keck Foundation.

* Corresponding author. Tel: (718) 430-3591. Fax: (718) 430-8819. E-mail: jfriedma@aecom.yu.edu.

10.1021/bi000536x CCC: $19.00
Published on Web 12/02/2000

of trapping and characterizing well-defined populations of nonequilibrium species such as the ligand binding intermediates.

Certain intermediates can be generated by photodissociating the fully liganded R state species (*14*). Time-resolved resonance Raman (*15*−*23*) and absorption spectroscopies (*14*, *24*−*28*) have contributed much to understanding the conformational changes that take place after rapid ligand dissociation of COHbA. This approach, while useful in terms of probing the tertiary and quaternary changes associated with the transition from the liganded R to deoxy T structures, does not provide a straightforward means of probing other key intermediates such as the liganded or partially liganded T state species and the fully deoxy R species [as opposed to the early time photoproduct of liganded R which still retains the initial tertiary conformation of the liganded R state species (*15*−*17*, *19*)].

Encapsulation of proteins in porous sol−gels is a possible approach to generating many of these important intermediates that are not accessible through conventional time-resolved studies. It has been shown that many proteins can be encapsulated in porous sol−gels derived from tetramethyl orthosilicate (TMOS) with a retention of functionality and enhanced stability (*29*−*41*). The sol−gel matrix traps the protein, but both solvent and small solute molecules can diffuse into the sol−gel through a network of 50−100 Å diameter pores. These small molecules can bind to or react with the encapsulated protein molecules. Thus O_2HbA can be encapsulated, but the oxygen can still be removed by the addition of sodium dithionite. Similarly, encapsulated deoxygenated HbA (deoxyHbA) can become saturated with ligands (O_2, CO, or NO) when ligand is introduced into the solvent bathing the gel.

Pioneering measurements of oxygen binding and dissociation curves derived from encapsulated deoxy- and oxyHbA at 10 °C indicate an absence of cooperative ligand binding (*42*). The encapsulated deoxyHbA binds and releases oxygen with low affinity, consistent with the properties of a noncooperative T state species. In contrast, encapsulated O_2-HbA loses and rebinds oxygen with high affinity, in a manner consistent with a trapped R state species. This and subsequent studies (*43*−*47*) strongly suggested that the sol−gel locks in the quaternary structure of the initial encapsulated population. Thus, when deoxyHbA and O_2HbA are encapsulated, the T and R structures are maintained, respectively, even when the ligation status of the heme is changed.

The oxygen binding studies of sol−gel encapsulated hemoglobin raise the exciting prospect of using sol−gels to trap nonequilibrium species such as liganded T and deoxy R. A full analysis of the potential of this technique requires a more detailed probe of the functional, conformational, and dynamical behavior of the encapsulated proteins. Resonance Raman spectroscopy has been used to help determine the extent to which both tertiary and quaternary conformational changes are restricted in the sol−gel. Visible resonance Raman spectra of a deoxygenated sample of encapsulated HbA generated by adding dithionite to an encapsulated O_2-HbA sample reveal that both tertiary and quaternary structural changes are slowed as the sol−gel is cooled (*46*). A UV resonance Raman study (*47*) on encapsulated deoxyHbA exposed to CO reveals that at 4 °C the addition of CO minimally perturbs the quaternary or tertiary structure of the encapsulated T state HbA. Subsequent spectra obtained after allowing the sample to remain at ambient temperatures for a few hours indicate additional conformational changes reflecting T → R changes in the hinge region but not the switch region of the R−T-sensitive $\alpha_1\beta_2$ (and $\alpha_2\beta_1$) interface. These two Raman studies (*46*, *47*) clearly show that sol−gel encapsulation is a viable method for overcoming the diffusion and mixing time limitations in a typical rapid mix experiment.

A full molecular level picture of the sequence of events that occur during the course of a protein reaction requires not only the conformational aspects but also the corresponding functional parameters that can be correlated with structure. The Raman spectroscopy studies indicate that it is possible to follow conformational changes in the sol−gel. Oxygen binding curves are not an appropriate measure of reactivity during the evolution of structure within the sol−gel. This follows because of both the time required for equilibration during the measurements and the fact that the measurement gives model-dependent details of the ensemble of conformations without being able to easily evaluate the properties of the different populations. Ligand rebinding kinetics (*1*) are much more suitable as a probe of function under these nonequilibrium conditions. Kinetic traces can be generated faster, and the kinetic analysis allows for better separation of functionally distinct populations. Ligand rebinding kinetics from photodissociated liganded hemoglobins fall into two classes of phenomena schematized in the equation that follows: geminate rebinding (*24*, *25*, *48*−*50*) and solvent phase rebinding (*1*). Both are highly sensitive to conformation and solvent conditions.

$$\mathrm{COHb(R,\,T)} \underset{\substack{\text{geminate phase}\\(<1\ \mu\text{s})}}{\overset{+h\nu}{\rightleftharpoons}} \underbrace{\{\mathrm{Hb^*(R,\,T) + CO}\}}_{\text{geminate pair}} \underset{\substack{\text{solvent phase}\\(>100\ \mu\text{s})}}{\overset{\text{CO escape}}{\rightleftharpoons}} \mathrm{Hb(R,\,T) + CO}$$

When liganded hemoglobin is photodissociated, there is a period of time (<1 μs for solution phase samples in aqueous buffer) during which the photodissociated ligand remains within the protein. This composite species is often referred to as the geminate pair. The geminate pair can decay either by having the ligand escape into the bulk solvent or by recombining with the heme iron to which it was originally bound. Geminate recombination is the name given to this unimolecular rebinding process. The fraction of the photodissociated population that undergoes geminate recombination, referred to as the geminate yield (GY), is determined by the ratio of the rate of bond re-formation to the sum of the rates of ligand escape and of bond re-formation. If the ligand escapes from the protein into the bulk solvent, the subsequent rebinding, termed solvent phase recombination, now becomes a bimolecular process that depends on the concentration of both CO and Hb in the solvent.

In solution at ambient temperature the geminate yield and the rate of solvent recombination are both dependent upon the protein conformation to which the ligand rebinds. In solution geminate recombination can occur over a temporal window extending from a few picoseconds out to several hundred nanoseconds (*51*). This time scale is faster than the time scales (*17*, *23*) for quaternary relaxation (20 μs) and for large-amplitude tertiary relaxations (~1 μs). Thus for

geminate recombination, the protein conformation that determines the GY may still reflect the initial tertiary and quaternary structure of the starting liganded species. This conformationally unrelaxed structure is often referred to as Hb*. In the usual case of R state COHbA in solution, the appropriate designation would be Hb*(R), whereas if a liganded T state species were to be prepared, the geminately recombining species would be Hb*(T), reflecting the ligand binding induced changes within the T quaternary state.

The rate constant for solvent phase recombination is on the order of 2×10^6 M^{-1} s^{-1} for the R state and about a factor of 50 slower for the T state (*1*). The R and T state solvent processes are much slower than any tertiary relaxation events occurring after photodissociation. Under these conditions the conformations undergoing R and T state solvent phase recombination are designated Hb(R) and Hb (T), respectively, indicating the heme environment no longer retains the contributions to the tertiary structure induced by ligand binding within a given quaternary state (e.g., deoxy T → liganded T). For the fully deliganded species, Hb(R) and Hb (T) are also referred to as deoxyHb(R) and deoxyHb(T), respectively, the latter being the equilibrium deoxy form of HbA.

The R state GY for COHbA in solution at 25 °C is approximately 0.5 (*48*−*50*). Several studies indicate that the GY for hemoglobins is highly responsive to quaternary structure (*16*, *19*, *25*, *52*−*54*). In general, the GY decreases dramatically in going from an R state to T state form of a given hemoglobin. Using iron−metal hybrids (*25*), double pulse excitations (*53*), and mixed ligation states and allosteric effectors (*54*), it was inferred that the GY for T state COHbA is just a few percent. The GY has also been shown to decrease for R state liganded HbA when allosteric effectors are added (*52*, *55*). These results suggest that tertiary structure changes within the R state also influence the GY. An important objective of the present work is to establish whether the sol−gel encapsulation of HbA allows for the kinetic characterization of CO recombination to HbA locked in either the R or T quaternary conformation without resorting to either mutant forms, allosteric effectors, chemical modifications, or iron−metal hybrids.

The present study focuses on four objectives associated with ligand rebinding kinetics from encapsulated hemoglobin. These objectives are as follows:

1. Establish whether interpretable and useful kinetic traces can be obtained from sol−gel encapsulated hemoglobins. As part of this objective, it is necessary to determine whether optically well-behaved sol−gel encapsulated hemoglobin samples can be prepared that stand up to the laser pulse energies needed to generate a sizable photoproduct population.

2. Use rebinding kinetics to evaluate how well a given sol−gel preparative protocol "locks in" the initial equilibrium distribution of hemoglobin structures. This objective also includes the determination of the extent to which encapsulation perturbs the kinetic patterns observed in solution.

3. Develop a protocol for encapsulation that yields optical quality sol−gels that reproducibly and effectively lock in conformations of hemoglobin.

4. Use the sol−gel to obtain kinetic properties of non-equilibrium forms of HbA.

The results obtained in this study clearly show that these objectives are attainable; however, the degree to which the initial structure of the encapsulated protein is maintained or locked in depends on the encapsulation protocol.

MATERIALS AND METHODS

Preparation of the Sol−Gel Encapsulated HbA. Wet porous sol−gels were prepared using three different protocols. All three protocols are based on a proton-initiated hydrolysis/condensation reaction of tetramethyl orthosilicate (TMOS) (Acros Organics). In all cases the starting materials are liquids. The sequence of hydrolysis, condensation, and polymerization of the TMOS-based solutions forms tough gel samples, which adopt the shape of the container into which the starting materials were added. Potassium phosphate, Bis-Tris acetate, or Hepes buffers were used for the preparation of the sol−gels.

Protocols. Protocol 1 is similar to the one described by Akbarian et al. (*36*). This procedure is derived from the initial method for encapsulating proteins developed by Zink and co-workers (*29*, *39*) and Avnir and co-workers (*37*, *38*) and used by Shibayama and Saigo (*42*) and by Bettati and Mozarrelli (*43*) for their hemoglobin studies.

For the preparation of a typical sol−gel in any buffer, 125 μL of TMOS was mixed with 35 μL of a 0.005 M hydrochloric acid solution and then sonicated at 4 °C, as described in the literature. An aliquot of 230 μL of a highly purified HbA solution in 50 mM buffer was then added to the TMOS solution. The mixing of the components was performed by gently vortexing. Following the solution solidifying, which results in the formation of a shaped rigid gel, bathing buffer was poured into a container on top of the thin layer of silica gel. Initial samples were prepared on thin quartz disks. Subsequently, all samples were prepared as a thin 1−3 mm layer on a single surface of a standard 10 × 10 mm optical cuvette and sealed with airtight ribbed septa, through which gases and solutions could be introduced or removed. The buffer-immersed gels were stored at 4 °C for at least 12 h after preparation prior to carrying out further experiments. Although minor variations from the typical preparation protocol were present in the preparation of some of the samples, this range of variation did not noticeably affect the behavior of the HbA molecules inside these sol−gels.

Protocol 2 differs from protocol 1 in two aspects. Acid is not used in the initial hydrolysis step. Instead, an equal volume of pH 6.5 buffer is added to the TMOS. In addition, the initial sonication step in protocol 1 is replaced by a more gentle 30 s vortexing. Thereafter, an aliquot of hemoglobin in the same buffer, equal to the buffer volume initially added to the TMOS, is immediately added. The solidification time, prior to the addition of the bathing buffer, is typically from 10 to 40 min.

In protocol 1, the sonication step leads to the extensive hydrolysis of the TMOS, prior to the addition of the protein solution. In protocol 2 on the other hand, the gentle vortexing with an equal volume of buffer initiates a slow hydrolysis which proceeds in the presence of the added protein solution. It was observed that addition of a 50 mM Bis-Tris acetate buffer at pH 6.5 yielded both high quality gels and a gelation time that allowed introduction of the protein without having

to race against an excessively fast gelation phenomena. Therefore, this buffer was used in the preparation of most of the protocol 2 and 3 protein-encapsulated samples. Buffers at higher pH often caused solidification prior to the thorough introduction of the protein solution into the pregel mixture.

Protocol 3 is similar to protocol 2 with one difference: buffers used in the preparation of the sol−gel samples contained 25% glycerol by volume. It was found that higher concentrations of glycerol in the buffer significantly slowed the gelation time.

For each type of preparation, HbA can be introduced into sol−gels in any of its equilibrium forms. In this paper, samples of encapsulated CO or deoxy derivatives of HbA have been prepared. After the formation of the sol−gel, the initial HbA derivative can be altered by allowing ligands or reductants to diffuse into the porous sol−gel. Oxygen, carbon monoxide, or sodium dithionite are able to diffuse through the porous structure of sol−gel and cause variations in ligation and oxidation states for the encapsulated hemoglobin.

In the experiments described herein the following nomenclature will be used to describe the types of encapsulated substances. The protein enclosed within square brackets means that the protein is encapsulated in the sol−gel as part of the preparative step. The substances listed after the brackets are added to the sol−gel after the aging process and before the kinetic or spectroscopic measurements. Thus, the [deoxyHbA] + CO refers to the protein that was initially encapsulated as deoxyHbA and subsequently exposed to CO after an aging period of at least 12 h (in the presence of a bathing buffer). In contrast, [COHbA] refers to a sample that was initially encapsulated and aged as COHbA.

Dr. Manjula, head of the Hemoglobin Core Facility at AECOM, provided highly purified samples of HbA in appropriate buffers. These samples were prepared using a previously described procedure (*56*), and the purity was verified using HPLC.

The absorption spectra of the encapsulated Hbs were all very similar to the corresponding solution phase samples as previously reported (*42*). Absorption spectra were recorded before and after each kinetic measurement in order to determine the condition of the sample with respect to degree of oxidation and state of ligation. The absorption measurements revealed that no changes or degradation in the samples occurred over the course of the experiments. The most common problem detected through absorption measurements was the formation of oxy and occasionally met forms of Hb during the aging of [deoxyHbA] samples. For that reason attention was focused on keeping the samples in an anaerobic environment during the aging process. With care, the [deoxyHbA] samples could be maintained as completely deoxy for several days or even weeks.

Kinetic Measurements. The flash photolysis apparatus employed for the carbon monoxide (CO) rebinding rate experiments is based on pump−probe optical setup. The frequency-doubled output of a Nd:YAG laser (5−7 ns; Surelite & Minilite lasers, Continuum) at 532 nm and 2 Hz repetition rate served to photolyze the carbonmonoxyhemoglobin derivatives. Recombination of the CO was monitored by measuring the change in sample absorption at 441.6 nm (CW, HeCd laser, Liconix). The unfocused (∼2 mm diameter spot size at the sample) and attenuated (several mW) HeCd probe laser beam passed through the studied sample nearly collinear with an unfocused Nd:YAG beam (∼1 cm diameter spot size at the sample). The probe beam was separated from the 532 nm second harmonic generation of the Nd:YAG laser using a dichroic mirror. The energy of the photolyzing beam was between 0.3 and 1 mJ at the sample. The transmitted power of the probe beam was kept at appropriate levels within the desired linear response regime of the photomultiplier (2.2 ns rise time; Hamamatsu, Bridgewater, NJ) by using neutral density filters.

A single grating monochromator (638 L/mm grating; Varian, Sugarland) was used to minimize any detection of false nonprobing light signals. The light intensity at the exit slit of the monochromator was measured with a photomultiplier tube and amplified with a 95 MHz preamplifier (Comlinear Corp., Fort Collins, CO). The output from the preamplifier was measured by a 500 MHz digital oscilloscope (LeCroy 9534C, Chestnut Ridge, NJ), and the transient absorption signal was averaged for 1000 laser shots on three different time scales of 1 μs/division, 100 μs/division, and 50 ms/division. The averaged signal from the oscilloscope was collected using LabView (National Instrument) and processed using Origin 6.0 Professional (Microcal Software, MA) and Igor Pro software.

The survival probabilities (plotted as changes in optical density) took into account average transmission of the probe laser beam in the absence of photolysis and were all normalized to 1 at the maximum change induced by the photolysis pulse at the start of the kinetic trace. The kinetic traces were displayed on a log−log plot of survival probability of photoproduct versus time. Plotting the full kinetic trace for the rebinding of CO to photodissociated COHbA (using a nanosecond photolysis pulse) on a log time axis allows for a clear separation among the three rebinding processes: geminate rebinding, R state solvent rebinding, and T state solvent rebinding. In addition, the relative amplitudes of the different phases help to provide details as to the effective viscosity experienced by the protein and the fraction of R and T species contributing to the kinetics. If, as is often done (*57*, *58*) when monitoring kinetics at cryogenic temperatures, a log−log plot is used (log survival probability of photodissociated heme versus log time), the kinetics of even a small population of a kinetically distinct species can be observed. Furthermore, on a log−log plot, exponential rate constants are easily approximated since exponential traces appear as horizontal lines that abruptly curve down and intersect the time axis at $1/k$, where the k is the rate constant in $\exp(-kt)$.

Samples were contained within a sample holder that allowed for controlled variation in temperature, 30 to −15 °C. The sample holder was housed within a Plexiglas chamber hooked up to a continuous flow dry nitrogen purge. This sample arrangement allows optimum minimization of complications due to condensation on the optical windows of the cuvette at subambient temperatures.

The position of the illuminated volume on the sample was not changed during the flash photolysis measurements. However, different spots were probed to test for sample homogeneity. The transient absorption kinetic traces showed no signs of sample degradation or alteration with variation of the photolysis pulse energies over the range of 30%, although explicit dependence on the energy of the photolysis pulse will be reported elsewhere.

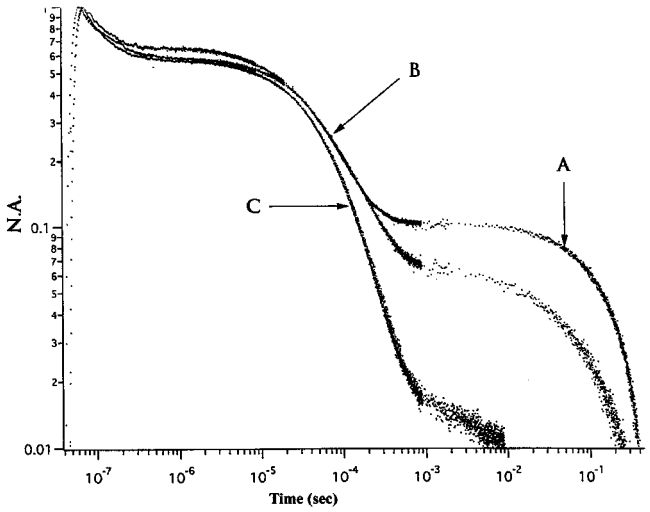

FIGURE 1: Kinetic traces (log−log plot of normalized absorbance versus time) of CO rebinding to hemoglobin at 25 °C after photodissociation of COHbA using a 7 ns, 532 nm excitation pulse: (A) encapsulated COHbA ([COHbA]) prepared using protocol 1; (B) solution phase COHbA; (C) [COHbA] prepared using protocol 2.

RESULTS

Figure 1 shows the kinetic traces at 25 °C for the ligand rebinding to photodissociated COHbA (trace B) in solution and in two different sol−gel matrixes (traces A and C). The solution phase sample exhibits three well-separated kinetic phases. The fastest rebinding process occurring between 10 ns and 1 μs is the geminate phase. The rebinding occurring between approximately 50 μs and 1 ms corresponds to the R state solvent phase bimolecular rebinding observed in solution and the slowest phase occurring between 10 and 100 ms overlaps in time with the T state solvent phase rebinding observed in solution. The solvent phase rebinding kinetics from $\alpha\beta$ dimers of HbA are similar to those from the R state tetramer. At the concentrations of COHbA typically used in this study ($\geq$0.5 mM in heme), the kinetics are reflective of the tetramer. Lowering the protein concentration by up to a factor of 3 had very little impact on the kinetics for the different phases. The higher concentration regime was used to provide adequate signal-to-noise ratios.

The two sol−gel encapsulated COHbA samples, [COHbA], used to generate the kinetics seen in Figure 1 were prepared using two different preparative protocols. Protocol 1, the standard protocol described in the literature, was used for the sample displaying the kinetics in trace A. It can be seen that the geminate phase is comparable to the solution sample but there is actually an increase in the relative fraction of T state solvent rebinding relative to trace B. Trace C, derived from an encapsulated sample prepared using protocol 2, shows a reduction in the T state solvent phase rebinding.

After preparing and running many encapsulated samples using either protocol and varying many of the preparative variables including aging time (hours to weeks), ratio of water to TMOS, drying time (from no drying to days), and pH (from 6.5 to 8), it is found that the two kinetic traces, A and C in Figure 1, represent two limits, with all of the different samples yielding traces that fall within those boundaries. Unfortunately, there is no discernible systematic dependence of the kinetic traces on the preparative protocol.

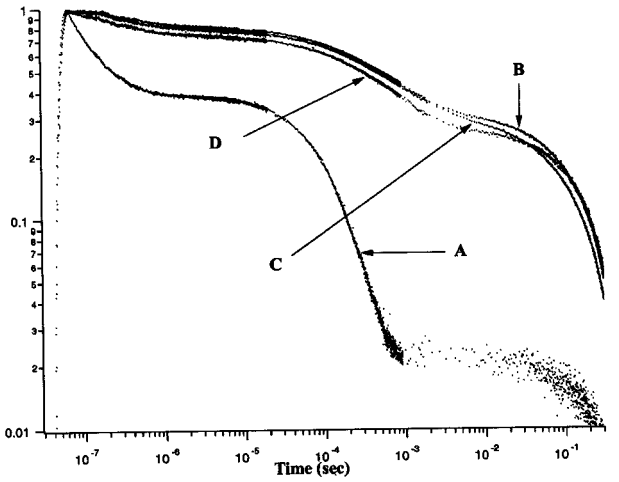

FIGURE 2: Kinetic traces (log−log plot of normalized absorbance versus time) of CO rebinding to hemoglobin at 4 °C after photodissociation of COHbA using a 7 ns, 532 nm excitation pulse: (A) solution phase COHbA in pH 6.8 Hepes buffer; (B) [deoxyHbA] + CO at pH 6.8 prepared using protocol 1 but with double the standard buffer (Hepes) content (2:1 buffer−TMOS) in the sol−gel preparative scheme and a 4 h drying period prior to aging as a wet gel for several days; (C) [deoxyHbA] + CO prepared using protocol 1 and aged for 40 days as a wet gel but with a 15 min drying period; (D) [deoxyHbA] + CO prepared using protocol 1 with the 2:1 buffer−TMOS ratio and aged for 69 days with no drying. Samples were aged as deoxyHbA in a nitrogen environment at 4 °C. The kinetic measurements on the sol−gels were all made minutes after the addition of CO to the sample. Saturation with CO was confirmed using absorption measurements.

Most samples, especially those prepared using protocol 1, display kinetic traces that are closer to trace A and therefore contain noticeable T state contributions. A minority of samples prepared using protocol 2 display kinetic traces that contain less than 2% T state rebinding. It was anticipated, on the basis of the earlier oxygen binding studies, that samples of [COHbA] would consistently yield kinetics that reflected only R state species. The appearance of the T state solvent phase kinetics in many of the samples implies that these sol−gels are not fully locking in the initial R structures (the initial encapsulated COHbA population is assumed to be entirely R), thus allowing the R $\rightarrow$ T transition to occur after photodissociation.

Figure 2 shows several representative kinetic traces from [deoxyHbA] + CO samples prepared using different encapsulation protocols. In each case the kinetics are generated within 15−30 min of introducing CO to the aged [deoxyHbA] samples. The three [deoxyHbA] + CO samples exhibit similar traces (B, C, and D) that differ substantially from kinetic trace A from either aqueous samples of COHbA or [COHbA] samples as shown in Figure 1. In all three cases shown, there is a large reduction in the geminate yield (GY) and a large increase in the fraction of sample undergoing T state solvent phase rebinding. All three traces show an inflection between 100 μs and several milliseconds. The initial (vide infra) fraction of the photodissociated sample undergoing the T state solvent phase recombination and the faster solvent phase rebinding that comprises the inflection point populations could not be substantially changed as a function of initial aging time (for the [deoxyHbA]), drying time, or the water:TMOS ratio used in the initial preparation (prepared using protocol 1).

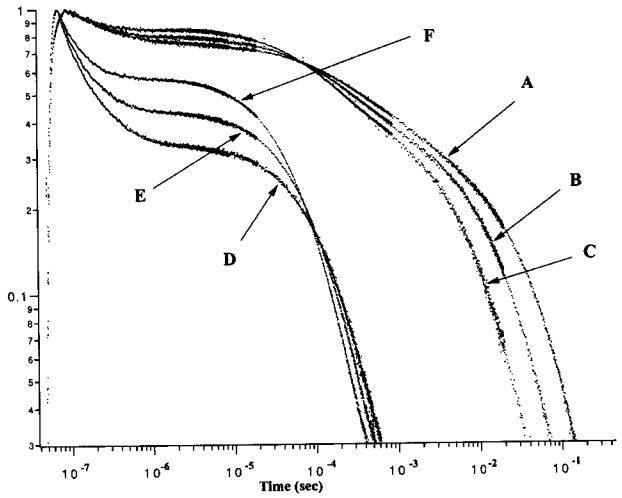

FIGURE 3: Temperature dependence of the kinetic traces for CO rebinding to photodissociated encapsulated COHbA. Traces A, B, and C are the rebinding traces for a [deoxyHbA] + CO sample at 4, 16, and 25 °C, respectively. Traces D, E, and F are the rebinding traces for a [COHbA] sample at 4, 16, and 25 °C, respectively.

Figure 3 shows the rebinding kinetics as a function of temperature for [deoxyHbA] + CO (traces A, B, and C) and [COHbA] (traces D, E, and F) prepared using protocol 1. It can be seen that the GY for both samples increases with a reduction in temperature. As occurs in solution, both the fast and slow solvent phases slow as the temperature is reduced. The [deoxyHbA] + CO sample shows solvent phase kinetics that are dominated by the slow T state solvent phase but also have, what appears to be, a contribution from faster kinetics that are closer to those observed for the [COHbA] sample.

The inflection hump at between 100 μs and several milliseconds noted above occurs in every kinetic trace derived from samples of [deoxyHbA] + CO prepared using either protocol 1 or protocol 2. Since this hump approaches the region of onset for the R state solvent phase rebinding, the obvious question arises as to whether it is a reflection of the sol−gel not completely locking in the initial deoxy T state structure when CO is first added.

Figure 4 shows the evolution of the kinetic trace of a [deoxyHbA] + CO sample from the point (within 15−30 min) when CO was first added to the aged [deoxyHbA] sample (curve A) to a time point 15 days after that initial addition of CO (curve B). During the 15-day period the sample was maintained at 4 °C. Also shown are kinetics for a solution phase sample under similar conditions (curve C). It can be seen that, with aging, the GY increases and the fraction of fast solvent phase recombination increases at the expense of the slowest phase.

Figure 5 shows the evolution of the kinetic trace of two [deoxyHbA] + CO samples. In the first case, sample 1 evolves from the point (within 15−30 min) when CO was first added to [deoxyHbA] (curve A) to a time point 75 min (curve B), 12 h (curve C), and 110 h (curve D) later while being maintained at 20 °C (the sample is cooled to 4 °C for each kinetic measurement). The effect of added heating on the evolution of the kinetic traces is seen in curves E and F, where subsequent to the addition of CO to the initial [deoxyHbA] the sample is maintained at 55 °C for a 12 h period prior to generating the kinetic trace (at 4 °C). Also

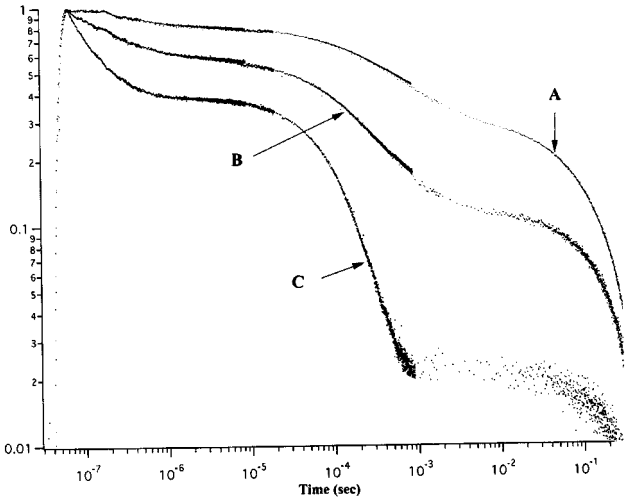

FIGURE 4: Evolution of the kinetic trace from a [deoxyHbA] + CO sample with aging. (A) Kinetic trace from a [deoxyHbA] sample prepared using protocol 1 (pH 6.8 Hepes). The kinetic trace was generated within several minutes of adding CO to the [deoxyHbA] sample. (B) The kinetic trace from the same sample as in (A) but after aging for 15 days (at 4 °C) after the initial addition of CO. (C) Kinetic trace from a solution phase sample of COHbA (pH 6.8). All kinetic traces were generated with the samples at 4 °C.

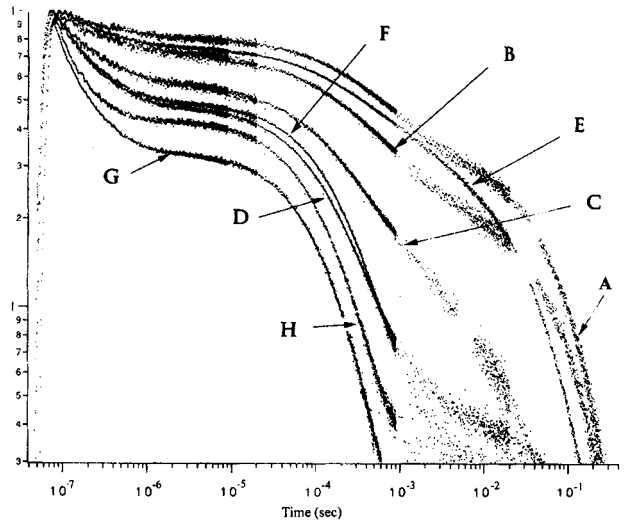

FIGURE 5: Evolution of the kinetic trace from two different [deoxyHbA] + CO samples with different aging times and protocols: (A) kinetic trace of [deoxyHbA] + CO sample 1 within minutes after the addition of CO; (B) kinetic trace from sample 1 75 min after the addition of CO with the sample maintained at 25 °C (kinetic measures of this over all samples were at 4 °C); (C) sample 1 kinetics after 12 h at 25 °C; (D) sample 1 kinetics after 110 h of aging at 25 °C; (E) sample 2 kinetics within minutes of adding CO; (F) sample 2 kinetics after 12 h of aging at 55 °C after the addition of CO; (G) kinetic trace from a [COHbA] sample; (H) kinetic trace from a solution phase sample of COHbA.

shown are kinetics for [COHbA] and COHbA solution phase samples (curves G and H, respectively) obtained under similarly cooled conditions.

Figures 4 and 5 show how, as the [deoxyHbA] + CO sample ages, both the GY and the fraction of the faster solvent phase recombination increase at the expense of the slow solvent phase. Warming the [deoxyHbA] + CO sample clearly accelerates the rate at which both the GY and the fast solvent phase increase in amplitude as seen in Figure 5. It can be seen that the kinetics generated by either warming

the sample (curve F) or waiting for a longer period at lower temperatures (curve D) result in similar kinetic traces that do not follow those obtained from either the [COHbA] sample or the solution phase sample. Even for the warmed or aged [deoxyHbA] + CO samples that show the most evolution toward the kinetics seen for the [COHbA] sample, the GY is still almost 20% lower despite the presence of only 5% slow solvent phase kinetics. In addition, the fast solvent phase kinetics for the relaxing [deoxyHbA] + CO samples are consistently slower than those of the COHbA solution and [COHbA] samples. The solvent phase kinetics observed for the partially relaxed samples (B and C) do not appear to be composed of a simple linear combination of the standard fast R and slow T kinetics observed in solution.

To better resolve the kinetic populations trapped within the gel, [COHbA] and [deoxyHbA] + CO samples were soaked in solutions containing high concentrations of CO-saturated glycerol. If glycerol can diffuse into the pores of the sol−gel and access the Hb, then it should be possible to increase the effective viscosity. The nature of the sol−gel sample allows for a rather straightforward change of solvent including the addition of a large excess of concentrated glycerol solutions.

The introduced glycerol, if it does indeed diffuse into the sol−gel resulting in an equilibration between the bulk solvent and the pores of the sol−gel, can be anticipated to induce the usual viscosity effects observed for the ligand rebinding kinetics. These will include an extension of the geminate phase due to a damping of the fluctuations that lead to ligand escape from the protein (*57*, *58*) and effects due to inhibition of relaxation dynamics such as quaternary and tertiary relaxations (to the extent that they are still occurring in the gel) that occur on the time scale of the kinetic measurements (*28*, *59*−*66*). Extending the geminate phase and damping the conformational relaxation should expose distinct noninterconverting kinetic populations locked in by the glycerol saturated sol−gel.

Figure 6 shows the effect of added glycerol on the rebinding kinetics for [COHbA] and for [deoxyHbA] +CO samples prepared using protocol 1 (similar results were also obtained using protocol 2). Glycerol clearly enters the sol−gel and influences the ligand rebinding kinetics. In both instances the geminate phase is extended and is exhibiting a near-linear time dependence on the log−log plot as is observed for COMb and COHb at either cryogenic temperature or high viscosity levels exceeding several hundred centipoises. For [COHbA] it can be seen that the replacement of the bathing buffer with CO-saturated glycerol results in an increase in the GY from ∼65% to 92% and extends the geminate phase out to beyond ∼10 μs. There is corresponding decrease from 30% down to 0.08% in the fraction of photodissociated molecules undergoing the solvent phase rebinding. A slowing of the solvent phase kinetics occurs as is anticipated for an increase in the bulk solvent viscosity.

The effect of added glycerol on the [deoxyHbA] + CO sample is more complex than for the [COHbA] sample. As with the [COHbA] sample, glycerol greatly extends the geminate phase. At −10 °C, the geminate phase in the presence of 80% glycerol persists to nearly 100 μs and the GY is increased from ∼20% to ∼60% (trace D). The increase in the GY comes not at the expense of the slow T state solvent phase rebinding but almost completely at the expense

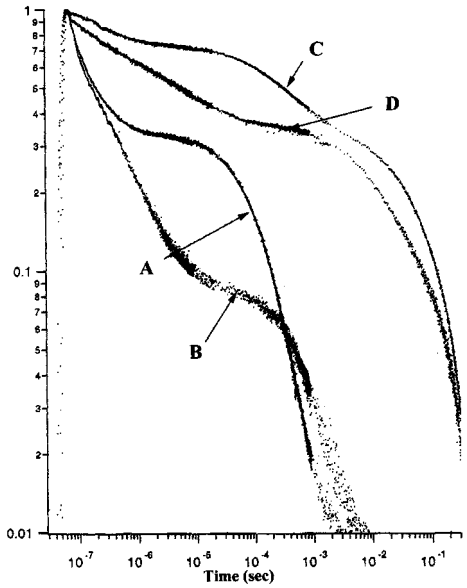

FIGURE 6: Effect of added glycerol on the rebinding kinetics of sol−gel encapsulated COHbA: (A) the kinetic trace from a [COHbA] sample immersed in pH 7.4 buffer; (B) the kinetic trace from the same sample as in (A) but with the buffer replaced with 100% glycerol; (C) the kinetic trace from a [deoxyHbA] + CO sample immersed in pH 6.8 buffer; (D) the kinetic trace from the sample used for (C) but with the aqueous buffer replaced with a buffer (pH 6.8) that is 80 vol % glycerol. Traces A, B, and C were all generated at 4 °C whereas trace D was generated with sample at −10 °C.

of the population undergoing the faster solvent phase rebinding that gives rise to the inflection hump at ∼100 μs.

The glycerol results clearly indicate that when either protocol 1 or protocol 2 is used to prepare [deoxyHbA] + CO, the resulting sample contains at least two kinetically distinct populations. As noted above, attempts at increasing the fraction of COHbA that rebinds with kinetics consistent with the low-affinity T state by varying aging time (hours to weeks), drying time (up to several days), and the TMOS:water ratio within the parameters of protocol 1 or 2 resulted in minimal variation from the pattern seen in Figure 2. This observation on the [deoxyHbA] + CO samples and the observation that many of the [COHbA] samples display kinetics that contained a few percent T state solvent phase rebinding indicate that Hb samples encapsulated using protocol 1 or 2 do not become fully locked into their initial distribution of solvent-based structures. A small fraction of the encapsulated COHbA sample can undergo the R to T transition, and a clearly discernible fraction of the encapsulated deoxyHbA sample becomes a distinct higher affinity population when CO is added.

In an attempt to improve the locking-in capability of the sol−gel, a different preparative protocol was used for encapsulation. Protocol 2, which combines the hydrolysis and condensation steps by eliminating the initial sonication step, was modified to include the initial addition of buffer containing 25% glycerol (protocol 3). The same protocol was also tried with protocol 1; however, Raman studies on myoglobin (Peterson and Friedman, unpublished results) indicate that this variation did not result in as good a conformational "lock". The glycerol-containing buffer was used in all aspects of preparation of the sol−gel including the initiation of hydrolysis and condensation. The hemoglobin

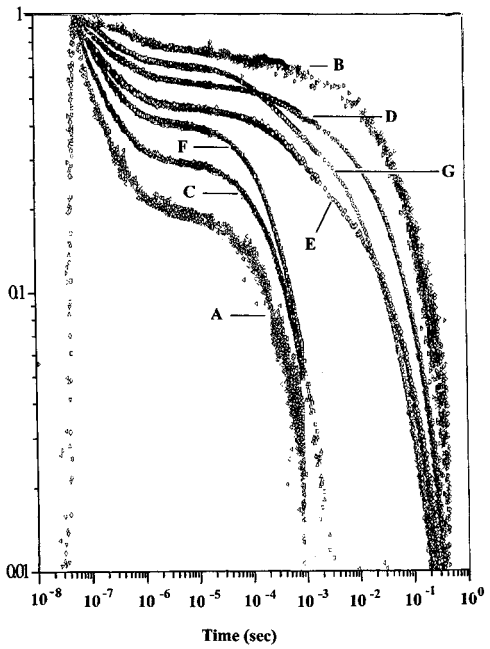

FIGURE 7: Kinetic traces of encapsulated COHbA as a function of preparative protocol. Traces A and B were derived from protocol 3 samples (pH 6.8 Bis-Tris acetate) of [COHbA] and [deoxyHbA] + CO, respectively; traces C and D were derived from protocol 3 samples (phosphate, pH 6.8) of [COHbA] and [deoxyHbA] + CO, respectively; trace E was derived from a protocol 3 sample (pH 8 Hepes) of [deoxyHbA] + CO; traces F and G were derived from protocol 2 samples (Hepes, pH 7) of [COHbA] and [deoxyHbA] + CO, respectively. All measurements were made on samples maintained at 4 °C. The traces derived from [deoxyHbA] + CO samples were all made within several minutes of adding the CO to the [deoxyHbA] samples. Kinetic trace B did not show the evolution with time (several days) seen for the protocol 1 and 2 samples when maintained at 4 °C.

solutions were similarly prepared using buffers containing 25% glycerol. The kinetic traces (not shown) from photodissociated COHbA and COMb in these 25% glycerol solutions are not noticeably different from those derived from the glycerol-free solvent. Thus any change in the kinetics using protocol 3 is not due to the minimal viscosity effect arising just from the 25% glycerol in solution but from glycerol-induced changes in the properties of the sol−gel.

Figure 7 compares kinetic traces from [COHbA] and [deoxyHbA] + CO encapsulated using protocols 3 and 2. Traces A and B are derived from [COHbA] and [deoxyHbA] + CO, respectively, prepared with pH 6.8 Bis-Tris acetate buffer using protocol 3. Traces C and D are derived from [COHbA] and [deoxyHbA] + CO, respectively, prepared with pH 6.8 KP buffer using protocol 3. Trace E is derived from a [deoxyHbA] + CO sample prepared using protocol 3 with pH 8 Hepes buffer. The corresponding trace for the [COHbA] sample prepared under the same conditions is virtually identical to trace C and is therefore omitted from the figure. Traces F and G are derived from [COHbA] and [deoxyHbA] + CO, respectively, prepared with pH 7 Hepes buffer using protocol 2.

Figure 7 shows several trends. With respect to the traces derived from the [COHbA] samples, the addition of 25% glycerol (protocol 3) substantially increases the GY, with the largest increase occurring for the pH 6.8 Bis-Tris acetate buffer. The [deoxyHbA] + CO samples also show a range of values for the GY, with the Bis-Tris acetate protocol 3 sample showing the lowest value. The traces (traces B and D) from samples of [deoxyHbA] + CO prepared using protocol 3 at pH 6.8 do not show the 100 μs inflection hump seen for the protocol 1 and 2 samples (Figures 2−5, trace G in Figure 7). It can be seen that the inflection hump does reappear for the high pH protocol 3 sample (trace E). Recent measurements (Samuni and Friedman, unpublished results) show that, upon aging, protocol 3 pH 6.8 Bis-Tris acetate samples of [deoxyHbA] + CO still exhibit the progressive increase in the GY seen for the protocol 2 and 3 samples (Figures 4 and 5); however, the rate is dramatically slower and the extent of relaxation much less.

There is some modest variation for the pH 6.8 Bis-Tris acetate protocol 3 [deoxyHbA] + CO samples both in the geminate yield which ranged from <10% to ∼20% at 4 °C and in the amplitude of the slow solvent phase rebinding. It is observed that the addition of IHP (4−6-fold excess over tetramer concentration) both to the initial deoxyHbA stock prior to encapsulation and to the buffer bathing the sol−gel results in samples consistently exhibiting kinetic traces with the lowest geminate yield and the largest amplitude for the slow solvent phase rebinding (similar to what is shown in trace B in Figure 7).

DISCUSSION

CO Rebinding Kinetics in Sol−Gel Encapsulated CO-HbA: Comparison with Solution Phase. The rebinding kinetics for photodissociated COHbA in the sol−gel are readily identifiable on the basis of a comparison with solution phase results. Although the different kinetic phases within the encapsulated sample are unambiguously assignable to well-characterized solution phase kinetics, the amplitude and time course of the kinetics are dependent upon the history of the sample. The most significant factor is whether the encapsulated COHbA was prepared by first encapsulating COHbA or by first encapsulating deoxyHbA and then adding CO after a period of aging (12 h to several days). The specific gelation protocol, the temperature and temperature cycling, and the composition of the bathing solvent (including the addition of cosolvents) all had a less dramatic influence on the kinetics.

Geminate Rebinding in the Sol−Gel. The geminate rebinding of CO to sol−gel encapsulated HbA is dependent upon preparative details. A comparison of the geminate rebinding from [COHbA] samples and solution phase samples indicates that, for protocols 1 and 2, the time scales for the geminate phase are similar and the GY is either comparable or slightly enhanced for the encapsulated samples. This result indicates that, for these sol−gels, the internal environment surrounding the Hb molecules does not significantly perturb the thermal fluctuations responsible for ligand escape. These fluctuations are still responsive to the usual viscosity effects observed when high concentrations of glycerol are added. The implication is that, with respect to these fluctuations, the effective viscosity imposed by the sol−gel on Hb is not especially high. In contrast, the geminate rebinding in the [COHbA] samples prepared using protocol 3, which has the added 25% glycerol incorporated into the sol−gel matrix, does persist slightly longer than for solution phase samples. The likely explanation for this behavior is that the incorporated glycerol imparts to the sol−

gel a higher effective viscosity with respect to conformational fluctuations leading to ligand escape.

The GY for the encapsulated hemoglobins shows considerable variation. The most substantial preparative factor impacting the geminate process is whether the photodissociated sample was initially prepared as [COHbA] or [deoxyHbA] + CO. In general, the GY for the former class of samples is much greater than for the latter.

It was mentioned in the introduction that the GY decreases in going from R state to T state species. Similarly, tertiary relaxation within the R state subsequent to photodissociation is claimed to progressively increase the barrier for geminate recombination (*12*, *15*). Conversely, a slow down in the tertiary relaxation due to either viscosity effects (*15*, *28*, *59*−*66*) or mutations (*67*) will result in an enhanced geminate yield. A comparable effect for the T state has also been proposed (*15*, *16*, *19*). As with the R structure the T structure should manifest at least two tertiary conformations: the deoxy T and liganded T structures. The most R-like liganded T conformations should exhibit a higher GY than those closer to the extreme deoxy T conformation. In addition, as with the R state, the rate of relaxation of the liganded T conformation toward the deoxy T conformation after photodissociation should also play a role in determining the GY.

The extreme limits for the GY in the sol−gel occur for protocol 3 (pH 6.8 Bis-Tris acetate) where the GY for the [COHbA] and [deoxyHbA] + CO samples are maximized and minimized, respectively. These protocol 3 samples exhibit kinetic traces that exhibit what appears to be a single solvent phase. The [COHbA] and [deoxyHbA] + CO samples only display the R state and T state solvent phases, respectively. This result coupled with the observation that the effective viscosity for the protocol 3 samples is higher than for the other preparative protocols suggests that the extremes in the GY are associated with conditions that have locked in conformations that are at the extremes within the accessible conformational space of HbA. Thus for protocol 3, the geminate processes for [COHbA] and [deoxyHbA] + CO are probably determined by conformations that approach the unrelaxed Hb*(R) and Hb(T) conformations, respectively.

The lower values of the GY observed for [COHbA] samples prepared using protocols other than protocol 3 (Bis-Tris acetate, pH 6.8) are likely due in part to the greater degree of Hb*(R) → Hb(R) tertiary relaxation occurring during the geminate phase. The observation of a population undergoing T state solvent phase recombination in many of samples supports the claim that relaxation is occurring to a much greater degree in these samples compared to the protocol 3 samples.

The kinetic traces for the [deoxyHbA] + CO samples prepared using protocols other than protocol 3 (Bis-Tris acetate, pH 6.8) are not as straightforward to explain as for the corresponding [COHbA] samples. The increased GY (compared to the protocol 3 samples) and the presence of inflection in the kinetic trace might be accounted for by a mixed starting population consisting of COHbA(R) and COHbA(T), in which case the inflection in the kinetic trace would be due to solvent phase recombination to Hb(R). Alternatively, the observed geminate and solvent phase kinetics could arise from a population of relaxed COHb(T). This species would represent the most "R"-like conformation at the extreme high-affinity end of the distribution of accessible T state structures. In contrast, the protocol 3 samples are postulated to have a conformation approaching the most "T"-like extreme at the low-affinity end of the distribution of T state structures.

The kinetic trace obtained upon addition of the high concentration of glycerol indicates that the population(s) giving rise to the inflection and the geminate process does (do) not contribute significantly to the population exhibiting the T state solvent phase kinetics. This result shows that there is a locked-in mixture of the "normal" T state population (as seen with protocol 3) and a population of either COHb(R) or COHb(T). The pH 8 protocol 3 sample of [deoxyHbA] + CO shows both the largest GY (for the [deoxyHbA] + CO samples) and the largest amplitude for the "inflection hump" fast solvent phase (Figure 7, trace E). This observation is consistent with observations (A. Friedman and W. Englander, private communication) that at high pH the sol−gel loosens. This loosening would allow for a buildup of liganded T and possibly liganded R population. More detailed studies are currently being pursued to explore and test this model.

As noted in the Results section, the GY for the [deoxyHbA] + CO samples progressively increases with aging of the sample, and this aging effect is accelerated with increasing temperature. The aging effect reduces the differences in the GY between the [COHbA] and the [deoxyHbA] + CO samples; nonetheless, in these studies, the GY for these aged and warmed [deoxyHbA] + CO samples never quite reaches the levels observed for [COHbA] samples. This result suggests but does not conclusively prove that the increasing population is not the same as that occurring with [COHbA]. A reasonable hypothesis that requires further testing is that, for the [deoxyHbA] + CO samples, the kinetics are largely the result of a population arising from the following sequence of conformational transitions: Hb(T) → Hb*(T) → Hb(R) → Hb*(R). As we move from left to right in this sequence, the GY increases and the solvent phase recombination rate increases. The kinetics for the fresh protocol 3 samples would be derived largely from a population of Hb(T), whereas the kinetics from fresh protocol 1 and 2 samples are derived from a mixture of Hb(T), Hb*(T), and possibly some Hb(R) and Hb*(R). With aging, the fraction of Hb(T) decreases and that of Hb*(T), Hb(R), and Hb*(R) increases.

Conformational Determinants of Kinetics in the Sol−Gel. There is evidence both from the oxygen binding studies and from the spectroscopy studies that, within the sol−gel, conformational changes in hemoglobin are greatly slowed or even stopped. Thus the conformational distribution of the starting hemoglobin solution upon encapsulation is likely to be the dominant factor controlling structure-sensitive aspects of CO rebinding. Clearly, to the extent that it occurs within the sol−gel, relaxation after photodissociation can be expected to alter the kinetics that are anticipated on the basis of the initially encapsulated conformational distribution.

In the limit where the sol−gel completely locks in and maintains the initial distribution of protein conformations, the [COHbA] and [deoxyHbA] samples would be populated by predominantly liganded R [Hb*(R)] and deoxy T [Hb(T)] state species, respectively. Under these conditions, the question arises as to whether the gel environment perturbs either of these equilibrium distributions. Both visible (*46*) and UV (*47*) resonance Raman spectra of sol−gel encapsu-

lated HbA suggest that the encapsulated hemoglobin retains the same or close to the same structure as in free solution. If we assume that [COHbA] and [deoxyHbA] are samples populated with molecules having the standard liganded R and deoxy T state conformations, respectively, the issues with regard to the kinetics become (i) to what extent does the gel prevent the evolution of structure once CO is added to the [deoxyHbA] sample and (ii) after photodissociation, are there tertiary and/or quaternary conformational changes on the time scale of the observed kinetics?

The extreme limit for low yield of geminate rebinding and large amplitude for slow solvent phase kinetics is observed for [deoxyHbA] + CO when the sample is probed soon after the addition of CO and is maintained at temperatures below 10 °C. Under similar conditions, the UV resonance Raman spectrum reveals minimal conformational perturbation of the initial deoxy T state spectrum (*47*). All of these features indicate that the observed kinetics are characteristic of a species locked into the deoxy T state, i.e., Hb(T). Similarly, visible resonance Raman results (*46*) seem to indicate that the kinetics observed for [COHbA] can be reflective of a nearly unrelaxed liganded R state population. Both Raman studies also show that intermediate forms can be generated and characterized. The deoxy T → liganded R intermediate observed in the UV resonance Raman study (*47*) shows features that are consistent with the proposed (vide supra) Hb(T) species that could give rise to the faster phase solvent process observed for the [deoxyHbA] + CO sample prepared using protocols 1 and 2. Studies are underway in which the kinetics are generated for spectroscopically well-characterized samples in an attempt to unambiguously assign the ligand rebinding properties to specific populations.

CONCLUSIONS

The results obtained in this study clearly demonstrate that sol−gel encapsulated hemoglobin samples can withstand the pulse energies needed to generate informative nanosecond and slower kinetic data. This property in combination with the slowing or elimination of tertiary and quaternary relaxation within the sol−gel provides a means of probing the reactivity of nonequilibrium populations. This approach is used in the present study to generate, in a straightforward fashion, the geminate and solvent phase rebinding kinetics for both the T and R forms of CO-saturated HbA.

The ability of the sol−gels to limit conformational change is shown to depend on the preparative protocol. Thus, by using different sol−gel preparative protocols to vary the degree of relaxation, it is possible to prepare and functionally compare different nonequilibrium populations.

The present study also reveals that glycerol can diffuse into the sol−gels and increase the effective viscosity of the encapsulated protein. Using this approach, it is possible to significantly extend the geminate phase. The combination of such an approach with reduction in temperature will allow for future studies in which the distribution of kinetic barriers for both equilibrium and nonequilibrium states of liganded heme proteins can be compared.

Recent spectroscopic studies on sol−gel encapsulated hemoglobin indicate that the use of temperature to control the rate and extent of relaxation within the sol−gel provides a means to overcome the limitations of conventional rapid-mix experiments in probing the initial conformational changes occurring upon ligand or substrate binding. The kinetic results of the present study clearly indicate that it is also possible to use this approach to follow the evolution of functional properties during the time course of conformational change. The combination of spectroscopy with measurements of functionality (e.g., ligand rebinding kinetics) on sol−gel encapsulated proteins after the introduction of substrates or ligands is likely to be a powerful new method with which to expose operational mechanisms within wide categories of proteins.

ACKNOWLEDGMENT

The authors thank Drs. B. Manjula, S. Acharya, and R. Noble for providing purified solutions of HbA. J.M.F. thanks B. Friedman for technical assistance in preparing figures for this work.

REFERENCES

1. Antonini, E., and Brunori, M. (1971) in *Hemoglobins and Myoglobins in their Reactions with Ligands*, Elsevier, New York.
2. Dickerson, R. E., and Geis, I. (1983) *Hemoglobin Structure, Function, Evolution, and Pathology*, Benjamin/Cummings, Menlo Park, CA.
3. Shulman, R. G., Hopfield, J. J., and Ogawa, S. (1975) *Q. Rev. Biophys. 8*, 325−420.
4. Perutz, M. F., Fermi, G., Luisi, B., Shaanan, C., and Liddington, R. C. (1987) *Acc. Chem. Res. 20*, 309−321.
5. Perutz, M. F. (1989) *Q. Rev. Biophys. 22*, 139−236.
6. Ho, C. (1992) *Adv. Protein Chem. 43*, 154−312.
7. Ackers, G. K. (1998) *Adv. Protein Chem. 51*, 185−253.
8. Perutz, M. F., Wilkinson, A. J., Paoli, M., and Dodson, G. G. (1998) *Annu. Rev. Biomol. Struct. 27*, 1−34.
9. Eaton, W. A., Henry, E. R., Hofrichter, J., and Mozzarelli, A. (1999) *Journal name 6*, 351−358.
10. Perrella, M. (1999) *Chemistry 81*, 157−178.
11. Gibson, Q. H. (1999) *Biochemistry 38*, 5191−5199.
12. Henry, E. R., Jones, C. M., Hofrichter, J., and Eaton, W. A. (1997) *Biochemistry 36*, 6511−6528.
13. Gill, S. J., Doyle, M., and Simmons, J. H. (1989) *Biochem. Biophys. Res. Commun. 165*, 226−233.
14. Sawicki, C. A., and Gibson, Q. H. (1976) *J. Biol. Chem. 251*, 1533−1542.
15. Scott, T. W., and Friedman, J. M. (1984) *J. Am. Chem. Soc. 106*, 5677−5687.
16. Friedman, J. M. (1985) *Science 228*, 1273−1280.
17. Rousseau, D. L., and Friedman, J. M. (1988) in *Biological Application of Raman Spectroscopy* (Spiro, T. G., Ed.) Vol. III, pp 133−215, Wiley & Sons, New York.
18. Kitagawa, T. (1992) *Prog. Biophys. Mol. Biol. 58*, 1−18.
19. Friedman, J. M. (1994) *Methods Enzymol. 232*, 205−231.
20. Su, C., Park, Y. D., Liu, G., and Spiro, T. G. (1989) *J. Am. Chem. Soc. 111*, 3457−3459.
21. Rodgers, K. R., Su, C., Subramaniam, S., and Spiro, T. G. (1992) *J. Am. Chem. Soc. 114*, 3697−3709.
22. Rodgers, K. R., and Spiro, T. G. (1994) *Science 265*, 1697−1699.
23. Jayaraman, V., Rodgers, K. R., Mukerji, I., and Spiro, T. G. (1995) *Science 269*, 1843.
24. Hofrichter, J., Sommer, J. H., Henry, E. R., and Eaton, W. A. (1983) *Proc. Natl. Acad. Sci. U.S.A. 80*, 2235−2239.
25. Murry, L. P., Hofrichter, J., Henry, E. R., Ikeda-Saito, M., Kitagishi, K., Yonetani, T., and Eaton, W. A. (1988) *Proc. Natl. Acad. Sci. U.S.A. 85*, 2151−2155.
26. Sassarole, M., and Rousseau, D. L. (1987) *Biochemistry 26*, 3092−3098.
27. Goldbeck, R. A., Paquette, S. J., Bjorling, S. C., and Kliger, D. S. (1996) *Biochemistry 35*, 8628−8639; Esquerra, R. M.,

Goldbeck, R. A., Reaney, S. H., Batchelder, A. M., Wen, Y., Lewis, J. W., and Kliger, D. S. (2000) *Biophys. J. 78*, 3227−3239.
28. Huang, J., Ridsdale, A., Wang, J., and Friedman, J. M. (1997) *Biochemistry 36*, 14353−14363.
29. Ellerby, L. M., Nishida, C. R., Nishida, F., Yamanaka, S. A., Dunn, B., Valentine, J. S., and Zink, J. I. (1992) *Science 255*, 1113−1115.
30. Narang, U., Prasad, P. N., Bright, F. V., Ramanathan, K., Kumar, N. D., Malhotra, B. D., Kamalasanan, M. N., and Chandra, S. (1994) *Anal. Chem. 66*, 3139−3144.
31. Yamanaka, S. A., Sishida, F., Ellerby, L. M., Nishida, C. R., Dunn, B., Valentine, J. S., and Zink, J. I. (1992) *Chem. Mater. 4*, 495−497.
32. Wu, S., Ellerby, L. M., Cohan, J. S., Dunn, B., El-Sayed, M. A., Valentine, J. S., and Zink, J. I. (1993) *Chem. Mater. 5*, 115−120.
33. Dave, B. C., Dunn, B., Valentine, J. S., and Zink, J. I. (1994) *Anal. Chem. 66*, 1120A−1127A.
34. Edmiston, P. L., Wambolt, C. L., Smith, M. K., and Saavedra, S. S. (1994) *J. Colloid Interface Sci. 163*, 395−406.
35. McKiernan, J., Simoni, E., Dunn, B., and Zink, J. I. (1994) *J. Phys. Chem. 98*, 1006−1009.
36. Akbarian, F., Lin, A., Dunn, B. S., Valentine, J. S., and Zink, J. I. (1997) *J. Sol−Gel Sci. Technol. 8*, 1067−1070.
37. Braun, S., Shtelzer, S., Avnir, D., and Ottolenghi, M. (1992) *J. Non-Cryst. Solids 148*, 739−743.
38. Avnir, D., Braun, S., Lev, O., and Ottolenghi, M. (1994) *Chem. Mater. 6*, 1605−1614.
39. Dave, B. C., Miller, J. M., Dunn, B., Valentine, J. S., and Zink, J. I. (1997) *J. Sol−Gel Sci. Technol. 8*, 629−634.
40. Das, T. K., Khan, I., Rousseau, D. L., and Friedman, J. M. (1998) *J. Am. Chem. Soc. 120*, 10268−10269.
41. Zheng, L., and Brennan, J. D. (1998) *Analyst 123*, 1735−1744.
42. Shibayama, N., and Saigo, S. (1995) *J. Mol. Biol. 251*, 203−209.
43. Bettati, S., and Mozzarelli, A. (1997) *J. Biol. Chem. 272*, 32050−32055.
44. Shibayama, N., and Saigo, S. (1999) *J. Am. Chem. Soc. 121*, 444−445.
45. Shibayama, N. (1999) *J. Mol. Biol. 285*, 1383−1388.
46. Das, T. K., Khan, I., Rousseau, D. L., and Friedman, J. M. (1999) *Biospectroscopy 5*, S64−S70.
47. Juszczak, L. J., and Friedman, J. M. (1999) *J. Biol. Chem. 274*, 30357−30360.
48. Alpert, B., El Mohsni, S., Lindqvist, J., and Tfibel, F. (1979) *Chem. Phys. Lett. 64*, 11−16.
49. Duddell, D. A., Morris, R. J., and Richards, J. T. (1979) *J. Chem. Soc., Chem. Commun.*, 75−76.
50. Friedman, J. M., and Lyons, K. B. (1980) *Nature 284*, 570−572.
51. Olson, J. S., and Phillips, G. N. (1996) *J. Biol. Chem. 271*, 17593−17596.
52. Friedman, J. M., Scott, T. W., Fisanick, G. J., Simon, S. R., Findsen, E. W., Ondrias, M. R., and MacDonald, V. W. (1985) *Science 229*, 187−190.
53. Marden, M. C., Hazard, E. S., Kimble, C., and Gibson, Q. H. (1987) *Eur. J. Biochem. 169*, 611−615.
54. Marden, M. C., Kister, J., Bohn, B., and Poyert, C. (1988) *Biochemistry 27*, 1659−1664.
55. Campbell, B. F., Magde, D., and Sharma, V. S. (1984) *J. Mol. Biol. 178*, 143−150.
56. Manjula, B. N., Kumar, R., Sun, D. P., Ho., N. T., Ho, C., Rao, M., Malavalli, A., and Acharya, A. S. (1998) *Protein Eng. 11*, 583−588.
57. Austin, R. H., Beeson, K. W., Einstein, L., Frauenfelder, H., and Gunsalus, I. C. (1975) *Biochemistry 14*, 5355−5373.
58. Doster, W., Kleinert, T., Post, F., and Settles, M. (1993) in *Protein−Solvent Interactions* (Gregory, R. B., Ed.) Marcel Dekker, New York.
59. Findsen, E. W., Friedman, J. M., and Ondrias, M. R. (1988) *Biochemistry 27*, 8719−8724.
60. Agmon, N., and Hopfield, J. J. (1983) *J. Chem. Phys. 79*, 2042−2053.
61. Srajer, V., and Champion, P. M. (1991) *Biochemistry 30*, 7390−7402.
62. Ansari, A., Jones, C. M., Henry, E. R., Hofrichter, J., and Eaton, W. A. (1992) *Science 256*, 1796−1798.
63. Ansari, A., Jones, C. M., Henry, E. R., Hofrichter, J., and Eaton, W. A. (1994) *Biochemistry 33*, 5128−5145.
64. Hagen, S. J., Hofrichter, J., and Eaton, W. A. (1995) *Science 269*, 959−962.
65. Gottfried, D. S., Peterson, E. S., Sheikh, A. G., Wang, J., Yang, M., and Friedman, J. M. (1996) *J. Phys. Chem. 100*, 12034−12042.
66. Kleinert, T., Doster, W., Leyser, H., Petry, W., Schwartz, V., and Settles, M. (1998) *Biochemistry 37*, 717−733.
67. Peterson, E. S., and Friedman, J. M. (1998) *Biochemistry 37*, 4346−4357.
68. Tian, W. D., Sage, J. T., Srajer, V., Champion, P. M., Chien, E., and Sligar, S. G. (1996) *Biochemistry 35*, 3487−3502.

BI000536X